Lipids Coupled to Polyelectrolyte Multilayers: Ultraslow Diffusion and the Dynamics of Electrostatic Interactions

Liying Wang, Monika Schönhoff,* and Helmuth Möhwald

Max-Planck Institute of Colloids and Interfaces, D-14424 Potsdam/Golm, Germany

Received: February 18, 2002; In Final Form: June 13, 2002

The lateral diffusion in a model membrane consisting of phospholipid monolayers attached to a polymer cushion is studied by means of fluorescence recovery after pattern photobleaching (FRAP). The polymer support is formed by multilayers of oppositely charged polyelectrolytes prepared by layer-by-layer self-assembly. Lipid diffusion coefficients in layers in air are very small, on the order of $D \approx 10^{-12}$ cm^2 s^{-1}, indicating strong electrostatic coupling. Comparing phosphatidylcholine lipids with different chain orders (DMPC, DOPC) and phosphatidic acid (DOPA), it is found that the lipid headgroup determines the lateral diffusion, with negligible influence of the chain. The sign of the charge of the last polyelectrolyte layer does not influence D, which is attributed to lipid binding to extending loops of internal polyelectrolyte layers. The dependence of D on temperature can be described by an activation behavior with activation energies on the order of 10 kT. No hysteresis occurs between diffusion measurements during heating or cooling cycles. Slow kinetics of chain rearrangement are observed at high T. Despite strong electrostatic interactions at the internal interface, evidence of a large amount of molecular flexibility of the polymer chains in layers is provided. The activation energies for a zwitterionic headgroup are larger than for an ionic headgroup, consistent with interactions of the zwitterionic head with both positive and negative polymer segments.

Introduction

Phospholipid bilayers serve as model systems of biological membranes. In particular, for the fabrication of biomimetic systems, the incorporation of functional components such as proteins requires the attachment of the membrane to a soft surface. Whereas solid substrates are commonly used for experimental investigations of 2D layer systems, polymer cushions on solid substrates can provide a soft and hydrated surface to which lipid layers can be bound.[1−5] In the struggle to design model membranes or biosensor devices of lipid bilayers, which reproduce the lateral mobility of natural systems, the interactions, such as electrostatic, van der Waals, or covalent, induced in the bilayer/cushion interface are inescapable. When optimizing the stability and functionality of the bilayers, potential effects of these interfacial interactions on the properties and biological function of the membrane have to be considered. It is thus of great interest to obtain a general understanding of the local interactions at lipid/polymer interfaces. This will be useful in finding new assembly approaches and materials and in controlling the architectures and properties of model membranes.

So far, research in this field is rare because it is difficult to find suitable methods to determine interactions at internal interfaces. The lateral lipid diffusion coefficient can serve as a parameter characterizing the local interaction of the lipids with a supporting surface: For a range of different solid inorganic substrates, the diffusion of phospholipids was shown to be slightly reduced as compared to that of free layers.[6,7] Two previous studies have dealt with lipid/polyelectrolyte coupled layers, where lateral lipid diffusion was investigated in various solvent environment[8] and in water for mixtures of lipids.[9] In this work, we focus on the role of the electrostatic interactions. We vary the charges of the respective interacting groups (i.e., the lipid headgroup and the polymer segments present at the interface). The present studies are performed in layer systems in air such that the lipid layer is subject to a strong electrostatic interaction with the supporting layer.

An important issue for the interpretation of the data is the formation of a layer system, which is controllable on a molecular level and additionally provides stability. For the lipid layer, molecular control is achieved by using the Langmuir−Blodgett technique. The polymer cushion is prepared by layer-by-layer assembly, which is a versatile and well-defined way to design the local environment because it provides uniform layers of controllable thickness.[10] We vary the nature of the lipid headgroup by using zwitterionic phosphatidylcholine molecules or negatively charged phosphatidic acid.

Fluorescence recovery experiments have a long history in the study of the lateral diffusion of lipids; see, for example, refs 11−16. In our systems, because of the coupling at the lipid/polymer interface, very slow diffusion is expected. Therefore, a special design of a FRAP setup is employed. It makes use of holographic pattern bleaching under total reflection conditions (pattern TIR−FRAP). Employing this principle, diffusion coefficients in the range of 10^{-14} to 10^{-7} cm^2/s can be measured.[17] It is very beneficial for this work that the measurement range can be extended to below 10^{-12} cm^2/s, where we can now with high precision detect influences of preparation parameters, lipid type, temperature, and polyelectrolyte type.

Materials and Methods

Materials. The polycations used for multilayer preparation were poly(ethylenimine) (PEI, $M_w \approx 55\,000$, Aldrich) and poly(allylamine hydrochloride) (PAH, $M_w \approx 70\,000$, Aldrich). Poly-

* Corresponding author. E-mail: Monika.Schoenhoff@mpikg-golm.mpg.de. Phone: +49-331-567-9256. Fax: +49-331-567-9222.

10.1021/jp0256600 CCC: $22.00
Published on Web 08/14/2002

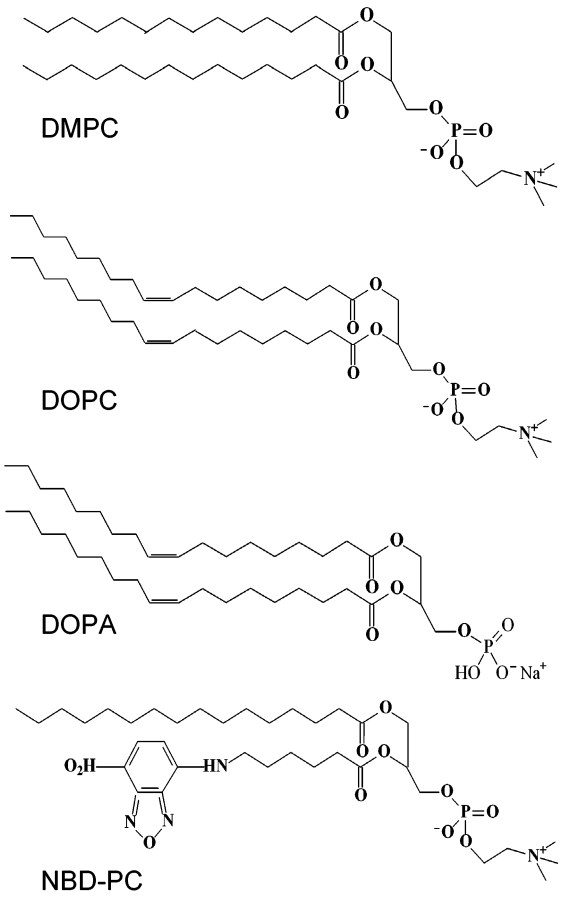

Figure 1. Chemical structure of the phospholipids used in this study. From top to bottom: DMPC, DOPC, DOPA, and NBD−PC.

(styrene sulfonate sodium salt) (PSS, $M_w \approx 70\,000$, Aldrich) was chosen as the polyanion. PSS was dialyzed against ultrapure water and freeze dried; the other polymers were used without further purification. The phospholipids used for monolayer formation are the zwitterionic 1,2-dimyristoyl-*sn*-glycero-3-phosphocholine (14:0 PC/DMPC), 1,2-di(*cis*-9-octadecenoyl)-*sn*-glycero-3-phosphocholine (DOPC), and the negatively charged phospholipid 1,2-dioleoyl-*sn*-glycero-3-phosphate (monosodium salt) (18:1 PA/DOPA); see Figure 1. The fluorescent probe 1-palmitoyl-2-[6-[(7-nitro-2−1,3-benzoxadiazol-4-yl)amino]caproyl]-*sn*-glycero-3-phosphocholine (16:0 to 06:0 NBD/PC) was added to all lipid solutions at a molar ratio of l%. All lipids and the dye probe were purchased from Avanti Polar Lipids Inc. except DOPC, which was purchased from Sigma (Germany). The water used in all preparation procedures was prepared in a three-stage purification system (Seradest) and had a resistivity higher than 18.2 MΩ cm.

Substrate Treatment and Polyelectrolyte Multilayer Preparation. Multilayer systems were prepared on different substrates using the method of layer-by-layer assembly.[10,18,19] Single-crystal silica wafers were first cleaned ultrasonically in 2-propanol for ca. 15 min and then, like quartz or glass microscope slides, were treated by the RCA procedure. This consists of immersing the slides in a mixture of H_2O, H_2O_2 (pa, 30% aqueous solution), and NH_4OH (pa, 28% aqueous solution) with a volume ratio of 5:1:1. The solution was heated to 70 °C for 20 min, followed by extensive rinsing with water. All of the substrates were completely hydrophilic after this cleaning process and were coated within 1 day. As a first layer, PEI was precoated to form a positively charged surface on the substrates by immersing them in a 10^{-2} M aqueous solution of PEI for 30 min. (All polymer concentrations given here refer to the monomer concentration.) After adsorption, samples were washed in water to remove excess polymer. After leaving the sample in air for 7 min, multilayers were fabricated by alternatingly immersing the PEI-coated substrates in polyanion and polycation aqueous solution for 20 min, beginning with anionic PSS. The adsorption processes were achieved in an automatic procedure. Aqueous solutions (10^{-2} M) of PSS or PAH containing 0.1 M NaCl (or 1.0 M NaCl, where indicated) were used. After each adsorption step, the substrates were rinsed in pure water for 3 min, and after adsorption of each PSS/PAH layer pair, the samples were kept in air for 7 min at ambient temperature.

The multilayer assemblies were characterized by small-angle X-ray scattering (STOE and CIE GmbH Darmstadt, Germany, $\lambda = 1.54$ Å (Cu Kα)) using samples prepared on silica. The film thickness was deduced by observing the Kiessig interference in X-ray reflectivity. The roughness of the multilayers on silica was determined by AFM (Digital Instruments, Santa Barbara, CA) and is less than 1 nm over an area of 1 μm × 1 μm. In addition, by using quartz substrates, the multilayer that was built up was controlled and confirmed by UV/vis spectroscopy (Varian Cary-5 UV/vis spectrophotometer).

Lipid Monolayer Deposition. Lipid monolayers were deposited by the Langmuir−Blodgett technique using a Langmuir trough (NIMA). The glass substrates precoated by multilayers of polyelectrolytes were first immersed in the aqueous subphase while a temperature of 20 ± 1 °C was maintained by a water circulating system. The lipid monolayers were obtained by the spreading of 10^{-3} M chloroform solutions of the lipid containing a l% molar ratio of the fluorescent probe onto the water surface. After 10 min, during which time the solvent was allowed to evaporate, the monolayer was compressed at a rate of 30 cm^2/min to a lateral pressure of 30 mN/m. While monolayers were transferred to the substrate at a rate of 1 mm/min, this pressure was maintained by an electronic feedback system. After deposition of the lipid monolayer, the samples were stored in clean containers at room temperature. Such layers, kept at ambient conditions, were shown to contain about 10−20 wt % hydration water.[20]

Pattern TIR−FRAP Setup. An argon ion laser (Innova 90-6, Coherent, Inc. Santa Clara, CA) generated the excitation beam at 488 nm, which was a suitable excitation wavelength for the NBD dye. A beam splitter provided two laser beams of equal intensity and the same polarization (see Figure 2, top view). This provides a maximum contrast in the interference pattern, which was formed at the measurement spot, where the focus of the beams was made to overlap by a lens. To achieve a sufficient signal-to-noise ratio, the experiment was performed under total internal reflection conditions, where only signal arising from the surface was detected. Both beams were coupled onto the glass through a prism at an angle of incidence above the critical angle of total reflection (see Figure 2, side view). Thus, the two beams were totally reflected at the glass surfaces, and the evanescent field was selectively exciting molecules in the surface layer. By bleaching and observing the sample under total internal reflection (TIR), background signals not originating from the interface could be eliminated, which resulted in an improved sensitivity of the setup. In the measurements, we used two interfering intense beams for photobleaching; subsequently, one of them is attenuated and used to monitor the bleached area during measurements. The laser beam was controlled via an electronic shutter (76995-M, Oriel Instruments).

In the measurement spot, both bleaching beams intersected at an angle α to form the interference stripe pattern. The period

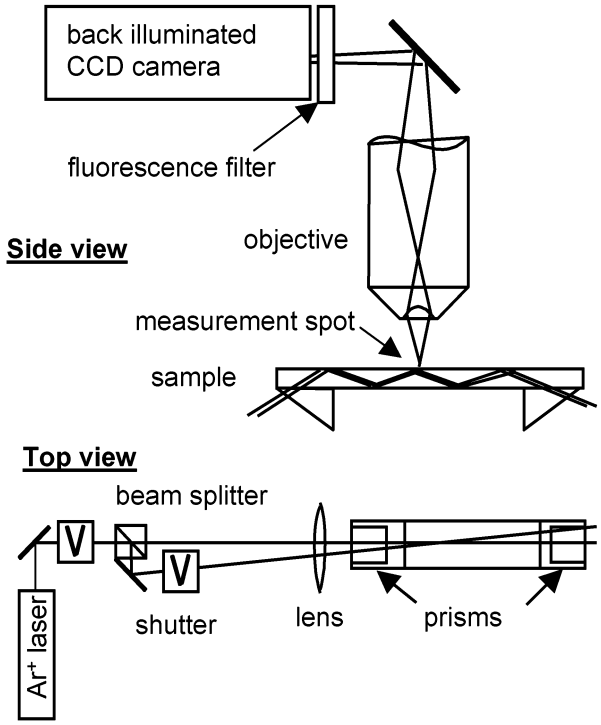

Figure 2. Schematic picture of the experimental setup.

of the pattern could be optimized for fast or slow diffusion by changing the angle α. A microscope objective(50×/0.50, LD, ZEISS) was used to collect the fluorescence emission from the sample and to project the pattern image onto the back-illuminated CCD camera (DV434-BV, ANDOR), which was cooled to −30 °C with the aid of a water-cooled thermoelectric element. A fluorescence filter (band-pass 515−565 nm) was positioned directly in front of the CCD detector head to prevent scattered excitation light from reaching the detector, thus decreasing the noise dramatically.

Through the objective and the projecting mirror, the pattern image was focused onto the camera chip such that the interference stripes were parallel to the long axis of the chip (column: 1024 pixels, row: 256 pixels). The stripe patterns were summed up along the columns (vertical binning) without losing any information. Since this operation was done directly on the CCD chip, it resulted in improved noise performance (see Figure 3c, d) compared to binning after readout because the readout process formed the main contribution to the noise. This procedure improved the signal-to-noise ratio and made it possible to measure signals of very low intensity.

For temperature-dependent measurements, a heating resistor was mounted below the sample and driven by a temperature controller (CAL 3200, CAL Controls Inc, U.K.). The temperature at the measurement spot was calibrated with a digital sensor (Schwille Elektronik, München) positioned on the measurement spot.

Image Acquisition and Analysis. The experimental parameters were as follows: laser power for bleaching, 0.8 W; laser power for bleached pattern observation, ∼0.05−0.1 W; exposure time, 0.1 s; interval between consecutive exposures, 20 s. Standard measurements were made at 20 ± 1 °C, and the temperature dependence was investigated in the range of ∼20−61 °C. The period of the pattern was adjusted to 4.0 μm, which was suitable for slow diffusion measurements. TIR−FRAP images taken before bleaching were used to confirm the homogeneity of the dye distribution (see Figure 3a). The image acquisition and the shutter were controlled by the CCD software.

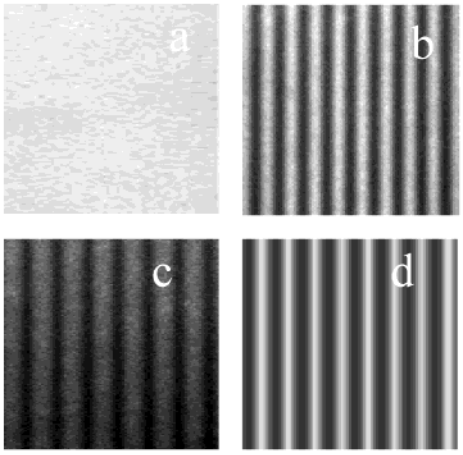

Figure 3. Fluorescence images of lipid monolayers deposited on the polyelectrolyte multilayers. The period of the pattern is 4 μm. (a) Homogeneous distribution of fluorescence taken with one beam (100 mW). (b) Pattern of stripes from interfering beams taken with two beams (200 mW). (c) Bleached pattern taken by irradiation with one beam (100 mW). (d) Same as (c) but with complete vertical binning on the chip.

Images were analyzed by Fourier transforms. After complete vertical binning (see Figure 3d), the intensity distribution of the interference stripes can be described by the intensity $I(x, t_i)$. Because the concentration of fluorescent molecules is very low, the fluorescence intensity is proportional to the concentration of unbleached probe molecules, $c(x, t_i)$. The 3D diffusion equation then simplifies to the 1D form:

$$\frac{\partial c(x, t)}{\partial t} = D \frac{\partial^2 c(x, t)}{\partial x^2} \tag{1}$$

Here, c is the concentration of the observed molecular species (i.e., the unbleached probe molecules), and D is the diffusion coefficient. A spatial Fourier transform of this equation leads to

$$\frac{\partial \tilde{c}(k, t)}{\partial t} = -Dk^2 \tilde{c}(k, t) \tag{2}$$

The solution of this equation is

$$\tilde{c} = \tilde{c}_0 \exp(-k^2 Dt) \tag{3}$$

Data evaluation is achieved by spatial Fourier transform of the pattern $I(x, t)$ as a function of time, yielding

$$\tilde{I}(k, t) = A_0 \exp(-k^2 Dt) + B \tag{4}$$

where A_0, D, and B are fit parameters. B corresponds to a nondecaying fraction of the stripe pattern and thus to an immobile fraction of the probe molecules. The mobile fraction of probe molecules was derived from the fit parameters. The diffusion coefficient can be calculated from the exponential fit of the following Fourier component decays: the component $\tilde{I}_1$ at $k = 2\pi/\lambda_{\text{pattern}}$ (λ_{pattern}: period of the stripe pattern) monitors the decay of the bleached pattern and provides a decay constant D_1 due to lateral diffusion. Because further bleaching during the measurement causes an additional decrease of $\tilde{I}_1$, which is due to a decrease of the total fluorescence intensity, a correction of the diffusion coefficient had to be included. This was done by extracting the Fourier component $\tilde{I}_0(k = 0)$, which corresponds to the time dependence of the total intensity and provides

a decay constant D_0 of the total intensity. The effective diffusion coefficient D is obtained as

$$D = D_1 - D_0 \tag{5}$$

In slow diffusion processes, overall bleaching of the sample is a factor that limits the detectable intensity and thus causes a low signal-to-noise ratio. The complete elimination of the bleaching effects induced by the monitoring beam enables the use of an excitation intensity that is high enough to allow the detection of weak fluorescence signals. In combination with the complete vertical binning, this allows the measurement of extremely slow diffusion coefficients as low as $D = 10^{-14}$ cm^2/s.

The initial concentration of the dyes does not need to be known to determine the diffusion coefficient. It is a parameter of a fitting function, but the diffusion coefficient obtained from the fit is independent of the initial concentration. From the representative image in Figure 3, one also deduces that inhomogeneities on the micrometer scale are immediately detected.

All of the diffusion coefficients presented in the Tables of this paper are average values from several measurements. Errors in D can arise from various sources. The fitting errors are less than 2% in all measurements and are thus negligible. Variations between different samples or different regions of one sample cause the largest error. Therefore, at least four different regions in one sample were measured and averaged. The experiments were done in air at ambient conditions, thus variations of the humidity (and thus the water content in the layers) might cause additional errors in the diffusion coefficient. For each system, different samples were prepared and measured on different days to confirm the average D value. The relative error for different measurements on one sample is less than 4%. The variation of the mean value of D obtained from different samples of identical composition and prepared under the same conditions is less than 10%. The D values represented in the Tables of this paper are averaged data from 4 to 8 measurements, and the error is estimated to 10%.

Results and Discussion

As an example, a typical measurement and the corresponding exponential fitting curves for DMPC coupled to 5*(PSS/PAH) layers in air are shown in Figure 4. I_0 gives the total intensity decay and I_1 provides the pattern decay. D_0 and D_1 are obtained according to eq 4. Because the experimental data can be fitted by a single-exponential decay, the experiment can be described by a single diffusion coefficient. In all experiments, I_1 does not decay toward zero (i.e., $B \neq 0$), which implies the presence of an immobile fraction of probe molecules. Such immobile fractions could arise from small immobile aggregates of dye. However, because the immobile fraction is rather low (3−15% in all experiments) and shows no systematic dependence on sample parameters, it is not discussed further.

The diffusion coefficients of lipids deposited on polyelectrolyte multilayers and measured in air are on the order of 10^{-13} to 10^{-12} cm^2/s and are thus several orders of magnitude lower than typical values obtained for lipid mono- or bilayers in contact with water ($\approx 10^{-8}$ cm^2/s); see, for example, refs 21 and 22. Water molecules can be expected to be present in layers kept at ambient conditions; however, the amount of water in polyelectrolyte multilayers is rather low (10−20 wt %).[20] In coupled lipid layers, such a low water content should result in a small distance between lipid headgroups and polymer segments. In fact, fluorescence resonant energy transfer (FRET) experiments show a very efficient transfer between the lipid layer and the last polyelectrolyte layer.[23] This proves the close proximity (<1 nm) of the lipid headgroup to the polymer charges in our system. Thus, our layers do not contain an interfacial water layer at the lipid−polymer interface and therefore differ from hydrated lipid layers at surfaces, where the thickness of an interfacial water layer influenced the diffusion.[24]

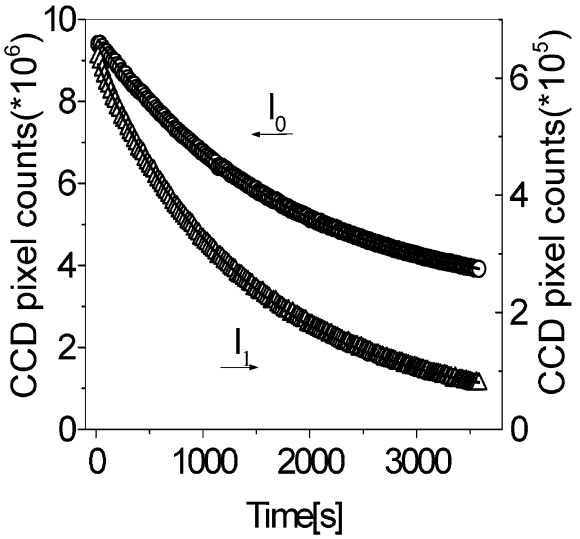

Figure 4. Decay of Fourier components I_0 and I_1 with time. The solid curves are exponential fits of the experimental data, resulting in the diffusion coefficient as explained in the text.

TABLE 1: Diffusion Coefficients of DMPC, DOPC, and DOPA on Five Double Layers of PSS/PAH in Air with PAH as the Outer Layer and on 5*(PSS/PAH) + PSS with PSS as the Outer Layer[a]

D (10^{-12}cm^2/s)	outer layer: PSS(−)	outer layer: PAH(+)
DMPC(±)	0.54 ± 0.05	0.60 ± 0.06
DOPC(±)	0.64 ± 0.03	0.52 ± 0.05
DOPA(−)	0.72 ± 0.07	0.65 ± 0.07

[a] Experiments were performed at room temperature (20 °C).

Headgroup Versus Chain Influence. Table 1 gives the diffusion coefficients for different lipid/polyelectrolyte combinations. It can be concluded that a strong electrostatic interaction due to the coupling of the lipid headgroups to the polyelectrolyte is present in all systems investigated. The diffusion of DMPC is the same within error when coupled to an outer layer of PAH or PSS; this implies a certain flexibility of the molecular arrangement at the headgroup−polymer interface.

The question of whether the lipid headgroup or the chain predominantly influences the diffusion can be answered by a comparison of different lipids. DOPC, which consists of a liquid chain with an unsaturated bond, shows the same coupling behavior as DMPC because the diffusion coefficients agree within error (see Table 1). The chain, therefore, does not have a large influence on the diffusion. However, upon investigating DOPA with a negatively charged headgroup, we found that the diffusion coefficients are slightly larger than for DMPC or DOPC. The negative headgroup appears to cause weaker binding to the polyelectrolyte layers. It is particularly surprising that the diffusion coefficients of DOPA coupled to a PAH or PSS outer layer differ only slightly, with the binding to PSS possibly being somewhat weaker, but D is the same within error. This implies that even in the case of an outer polyelectrolyte layer with a negative charge the negative lipid headgroup is subject

TABLE 2: Diffusion Coefficients of DMPC and DOPA on Multilayers Prepared at Different Salt Concentrations and with Different Polymers as the Last Layer, Determined at Room Temperature (20 °C)

composition	D (10^{-12}cm^2/s) 1.0 M NaCl	D (10^{-12}cm^2/s) 0.1 M NaCl
DMPC(±) on PAH(+)	0.66 ± 0.06	0.60 ± 0.06
DMPC(±) on PSS(−)	0.63 ± 0.05	0.54 ± 0.05
DOPA(−) on PAH(+)	0.71 ± 0.06	0.65 ± 0.07

to a strong attractive interaction. Repulsion, as expected between two negative layers, would increase the interlayer distance and subsequently cause a significant increase of the lipid diffusion coefficient. The findings can be explained only by the binding of the lipid headgroups to positively charged segments from the PAH layer beneath. The polymer obviously is flexible enough to provide positive segments on the multilayer surface, which cause binding of negatively charged lipids. Additionally, defects in the last layer can enable the lipid to bind to inner layers. This interpretation is in agreement with structural investigations of polyelectrolyte multilayers, where it was found that the internal roughness between subsequent monolayers is larger than the monolayer thickness (i.e., segments from one layer can extend through subsequent layers[25]). Furthermore, the outer layers of a polyelectrolyte multilayer assembly have been found to be more mobile and less condensed than the inner ones.[26] Because the system is swollen in water during the lipid-layer deposition, the outer layers can be considered to be mobile and, according to our results, can arrange in a conformation that provides the charge at the surface, which is necessary for an attractive interaction with the respective lipid headgroup charges.

Considering the lower diffusion coefficient of the phosphocholine lipids as compared to that of the acid, which implies stronger binding, we can speculate as to whether the zwitterionic headgroup can form bonds to both positive and negative polymer charges; this argument will be discussed in detail further below.

Variation of Polyelectrolyte Layer Thickness. To investigate the effect of increased polyelectrolyte mobility on the lipid coupling, the salt concentration in the polyelectrolyte solutions used in the multilayer preparation was varied. An increased salt concentration leads to a thicker layer,[27] and thus a higher mobility of segments in the outer layers can be expected. As determined from X-ray measurements, the thickness of one layer pair prepared using 1.0 M NaCl is 36 Å, which is larger than for a preparation from 0.1 M NaCl (26 Å). Table 2 gives the results for DMPC coupled to PAH or PSS as an outer layer. At the higher salt concentration of 1.0 M NaCl, slightly increased diffusion coefficients are indeed detected. The changes are not dramatic, in particular, in comparison to the errors, but a trend seems to be present. This can be interpreted as an enhancement of the lipid lateral motion by an increased mobility of the polymer chains in layers prepared with a high salt concentration.

Furthermore, the number of double layers of polyelectrolytes, N, was varied. Within the range of 2 to 10 double layers, no dependence of the diffusion coefficients on N is observed (data not shown). Five double layers of polyelectrolytes, or five double layers additionally covered with a PSS layer, respectively, are used as the polymer cushion in all of the following experiments, if not mentioned otherwise.

Temperature Dependence: (A) Kinetics. The effect of temperature on the diffusion is investigated for different lipid/polyelectrolyte combinations. The trend in the measurement shows an increase of the diffusion coefficients with increasing temperature. An interesting observation is that after heating a sample to a higher temperature, a time dependence of the diffusion coefficient occurs. This phenomenon is observed at temperatures above 45 °C in all lipid/polymer combinations investigated. As an example, Figure 5 gives diffusion coefficients of DMPC on 10*(PSS/PAH) determined in subsequent measurements after heating. The first experiment is started after the sample reached the target temperature. Each measurement takes 60 min, and the time interval between subsequent measurements at a given temperature is about 15 min, which is the time needed for adjustment. As shown in Figure 5, fast diffusion is observed at the beginning until equilibrium is reached, and a plateau with a slower diffusion occurs. If the heating resistor is removed after the experiment to let the sample cool to room temperature, the procedure can be repeated. Following the second or third heating process, the same time dependence of the diffusion coefficient is reproducibly observed, as the different curves in Figure 5 show. A possible explanation of the changes of D by a phase transition of the lipid layer was not confirmed because in the fluorescence images no lipid aggregates or domains are observed. Although the presence of nanodomains on the scale of <1 μm cannot be excluded because of the limited resolution, it seems unlikely that coupled lipids should form domains much smaller than typical structures observed in lipid phase transitions at the air/water interface (>1 μm). Thus, the change of the diffusion coefficient is not caused by a phase transition, and another interpretation of the above kinetic effect has to be put forward: A reversible equilibration of the sample after a temperature change can explain the data. Parameters that might be affected by a temperature increase are (a) the water content in the layers (hydration equilibrium) and (b) the polymer chain conformation because a rearrangement might follow the new hydration equilibrium. Concerning the water content, it can be expected that at an increased temperature there is less water present in the layers. This could explain the time dependence of the diffusion, which is fast directly after heating, corresponding to a strongly hydrated system, where the hydration water between lipid headgroups and polymer charges screens the interaction and facilitates lipid motion. Faster lipid diffusion was also found for the present layer systems, if swollen in water.[28] Thus, after heating, a decrease of the number of water molecules with time can lead to stronger binding and restricted mobility of the lipids and thus a reduced diffusion

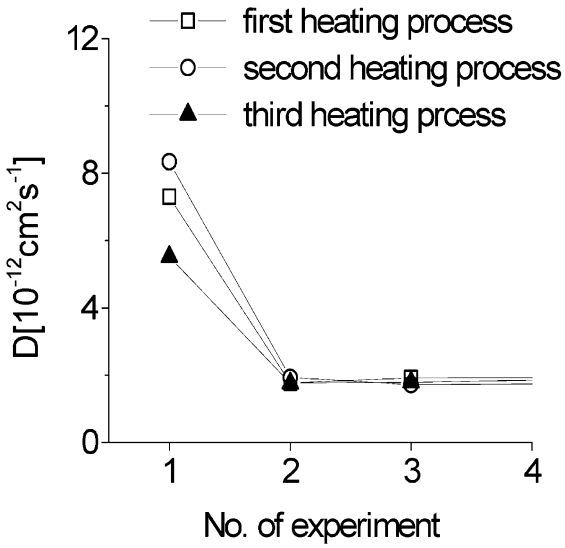

Figure 5. Change of the diffusion coefficient with time after raising the temperature.

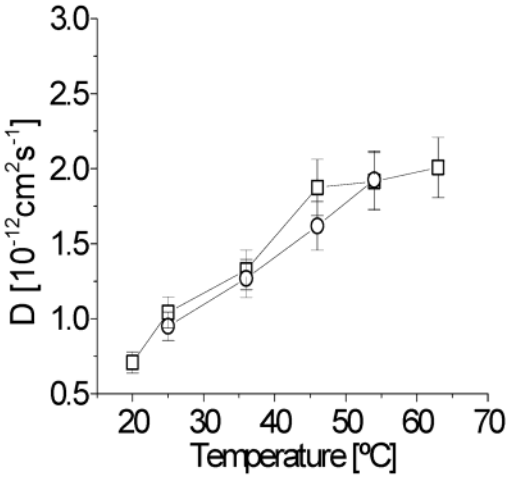

Figure 6. Reversibility of diffusion coefficients measured during stepwise heating (□) and cooling (○) of the sample for the layer system 5*(PSS/PAH) + PSS/DOPA.

coefficient. On subsequent cooling, water can be taken up again from the environment, resulting in reversible behavior.

However, it can be argued that the hydration equilibrium at elevated temperature should be reached in a short time because the water molecules are mobile and should evaporate faster than on the time scale of hours. Then the polymer will have to adjust to the change in hydration, and this process should exhibit a larger time constant than the hydration equilibrium, because a slow conformational relaxation of the polymer due to chain entanglement can be expected. A pronounced heating-induced shrinking of multilayered polyelectrolytes has also been observed in hollow shells created by the layer-by-layer assembly.[29]

In all of following experimental data, the plateau value of the diffusion coefficient after equilibration of the sample is evaluated.

Temperature Dependence: (B) Thermal History. Temperature-dependent diffusion experiments are performed by increasing the temperature stepwise and detecting several pattern decays at each temperature after equilibration to the plateau value of Figure 5. Figure 6 gives the diffusion coefficients as a function of temperature during heating (squares). The values are increasing with temperature. During subsequent cooling, the equilibrium diffusion coefficients at each temperature agree within error with the data taken during heating (i.e., no hysteresis or dependence on the thermal history is observed). It is not surprising to find this reversibility during a heating−cooling cycle because according to the results of Figure 5 the system is reversible with respect to heating and subsequent cooling.

In summary, it takes about 2 h for the sample to reach the new equilibrated coupling conditions after a change of temperature. Both the formation of a new hydration equilibrium and a rearrangement of polymer chains accompanying the hydration changes can occur in this period of time. The findings from the kinetic behavior further support the picture of pronounced molecular flexibility at the lipid/polymer interface, which is present despite very strong electrostatic binding.

Temperature Dependence: (C) Activation. Diffusion coefficients as a function of temperature are given in Figure 7 in the form of an Arrhenius plot for DMPC coupled to PAH or PSS as the last polyelectrolyte layer. Figure 8 gives the corresponding data for DOPA. For all systems investigated, the data agree with the assumption of an activation process

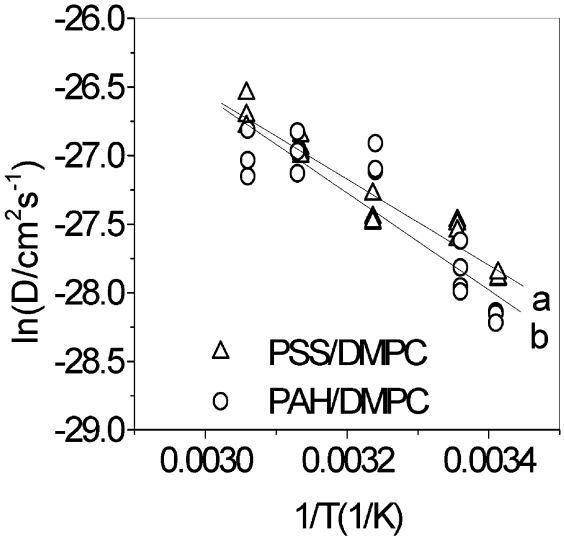

Figure 7. Arrhenius plot of the diffusion coefficients as a function of temperature for a DMPC monolayer on a PE multilayer system with PSS and PAH as the last layer. The straight lines are linear fits according to eq 6, from which the activation energy is extracted. Straight lines are fits of the data (a) for DMPC on PSS and (b) for DMPC on PAH.

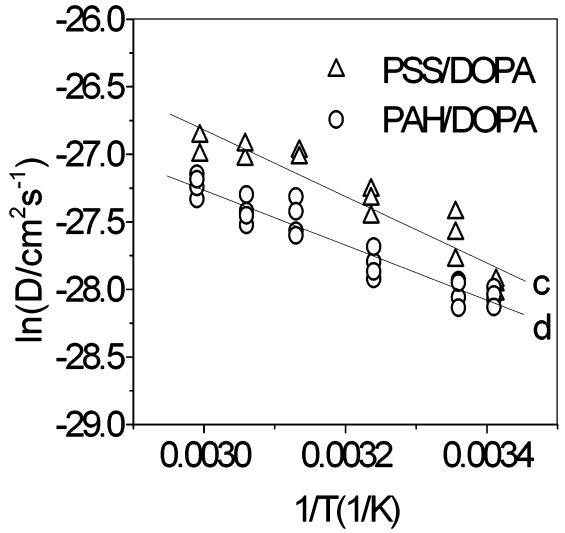

Figure 8. Arrhenius plot of the diffusion coefficients as a function of temperature for a DOPA monolayer on a PE multilayer system with PSS and PAH as the last layer. The straight lines are linear fits according to eq 6, from which the activation energy is extracted (c) for DOPA on PSS and (d) for DOPA on PAH.

controlling the lateral lipid mobility, as described by the equation

$$D = D^* \, e^{-\Delta E/kT} \qquad (6)$$

D is the diffusion coefficient at temperature T, ΔE the activation energy for diffusion, and D^* a preexponential factor.

Other authors have found phase transitions in DMPC-containing layers coupled to polymer cushions measured in water.[9,8,30] A sudden increase of the diffusion coefficient to the order of 10^{-8} cm^2 s^{-1} was observed on reaching the phase-transition temperature of DMPC (around 23.4 °C); this D value is characteristic for a fluid phase. In our experiments of coupled layer systems in air, no domain formation is observed, which would indicate the occurrence of a phase transition. The diffusion coefficient is continuously increasing with increasing temperature and remains very low. Within the error of the diffusion coefficients, all experiments can be interpreted in terms

TABLE 3: Activation Energies for the Diffusion of DMPC and DOPA Monolayers on Polyelectrolyte Multilayers Determined from the Slopes in Figures 6−8

activation energy (*kT*)	outer layer: PSS(−)	outer layer: PAH(+)
DMPC(±)	10.7 ± 0.7	12.1 ± 1.5
DOPC(±)	10.6 ± 1.6	
DOPA(−)	8.0 ± 0.9[a]	6.9 ± 0.5

[a] Determined as an average value from Arrhenius fits of the heating curve ($\Delta E = 8.4 \pm 0.9$) and the cooling curve ($\Delta E = 7.5 \pm 0.9$) in Figures 6−9.

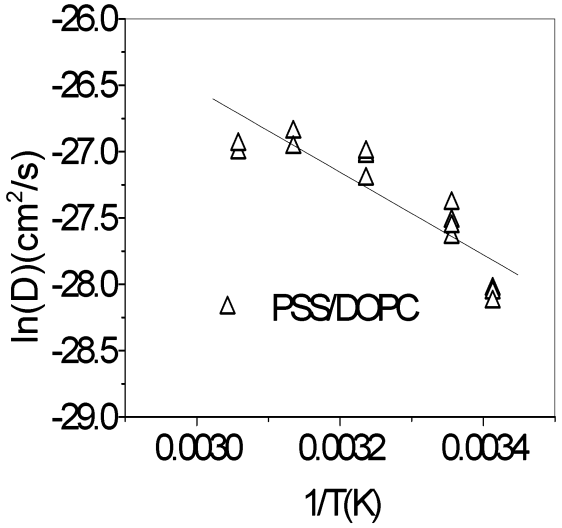

Figure 9. Arrhenius plot of the diffusion coefficient as a function of temperature for a DOPC monolayer on a PE multilayer system with PSS as the last layer. The straight line is a linear fit according to eq 6, from which the activation energy is extracted.

of an activation model. Activation energies are determined from the slope of a linear regression of ln*(D)* and are given in terms of *kT* (*k*: Boltzmann constant; *T*: room temperature, 293 K) in Table 3. All activation energy values are on the order of 10 *kT*.

Within the error determined from the fit of the corresponding Arrhenius plot, there is no difference between the activation energies of a lipid coupled to different polyelectrolytes in the last layers. Thus, the charge of the last polyelectrolyte layer is irrelevant not only for the diffusion coefficient, as discussed above, but also for the activation energy. This is further evidence of a flexible arrangement of positive and negative loops and tails at the polyelectrolyte multilayer surface.

After investigating the chain influence by comparing DMPC with DOPC (see Figure 9 and Table 3), we find that the activation energies for both lipids on PSS are the same within error, again proving a negligible influence of the chain on the lipid mobility. ΔE is, however, significantly lower for DOPA, again independent of the charge of the last polyelectrolyte layer. This can be attributed to a stronger immobilization of the zwitterionic headgroup. All of these relative differences between the systems that are investigated agree exactly with the findings for the room-temperature diffusion, as deduced before from Table 1.

Diffusion and Binding Energy. We conclude from all of the above results that the general picture of the coupled lipid−polyelectrolyte layer system shows that the headgroup and its interaction with the polyelectrolyte is the main factor determining the lipid mobility. In mobile bilayers, the lipid chain order is an essential parameter for lipid diffusion; see, for example, ref 31. The present system, however, involves strong electrostatic interactions in coupled layers. Furthermore, in air, the number of water molecules can be expected to be far lower than in hydrated systems; therefore, the interactions are less screened. In this regime of strong coupling, the lipid chain order appears to have a negligible influence on the lipid mobility. This would also suggest the independence of the diffusion on the lateral packing density. The latter is an important parameter in the free-area model, which is generally employed to describe lateral lipid diffusion.[32] In this model, the energy required for the formation of sufficient "free area" prior to a diffusion step of a lipid molecule is the limiting process determining an activation energy. In the present system, it can be assumed that the activation energy ΔE does not represent the energy for the formation of free area, which would depend on the chain packing, but rather the binding energy of the headgroups to the polyelectrolyte layer, which has to be overcome to cause diffusion. In the case of loose packing of the lipid chains and thus sufficient free area, the diffusion process can be described by a model of headgroup jumps between binding sites on the polyelectrolyte.[8] In such a picture, the binding energy, not the free area, is the limiting parameter for the diffusion process. By interpreting the activation energies of Table 3 as binding energies of the headgroups, they can, for example, be compared to adhesion energies of lipids to surfaces, which were determined by contact-angle measurements in wetting experiments of Langmuir monolayers: For a fully hydrated layer of DMPE on silica, adhesion energies are on the order of 0.6 to 3.5 kJ/mol,[33] whereas our results of $\Delta E \approx 10\ kT$ for polyelectrolyte-coupled layers correspond to about 24 kJ/mol. The difference of 1 order of magnitude can be attributed to the screening of the interactions in the hydrated layers investigated by Graf and Riegler, whereas in our layers, smaller hydration shells lead to a closer proximity and thus stronger electrostatic interactions of the charged groups.

The diffusion process in the layers is, however, not completely determined by the binding energies. Whereas the exponential factor in eq 6 accounts for the activation of the headgroup−polyelectrolyte interaction, the preexponential factor D^* can be interpreted as the frequency of attempts of the molecule to overcome the energetic barrier. From the activation energy of about 10 *kT*, eq 6 results in a D^* value of 10^{-8} cm^2/s. This value agrees well with the diffusion coefficient of a free, liquid membrane and thus accounts for the chain interactions and free-area effects, which are not contained in the headgroup coupling discussed above.

It is interesting that despite the interpretation of diffusion coefficients and activation energies in terms of local Coulomb interactions the ultraslow diffusion in coupled layers is still a collective process. Collectivity can be concluded because the NBD−PC molecule in DOPA layers acts as a probe for the DOPA−polyelectrolyte interaction instead of representing the NBD−PC− polyelectrolyte interaction, which would result in the same activation energies in PC or PA layers.

Polymer Flexibility. Vertical disorder in the polyelectrolyte layers causes positive and negative loops to provide binding sites at the surface, without detectable differences in the dependence of the sign of the charge of the last layer. Though it is known that polyelectrolyte multilayers generally exhibit a large roughness of the internal interfaces,[25] it is still surprising to find that positive and negative charges are equally accessible for the binding of lipid charges. However, in measurements of colloids coated with polyelectrolyte multilayers, the ζ potential generally shows a clear reversal of sign with the deposition of each layer and also shows large potential values (~50 mV).[34] These potentials prevent the adsorption of additional polyelec-

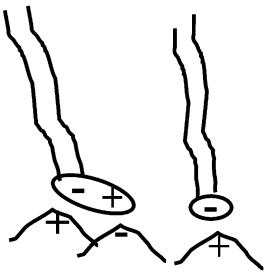

Figure 10. Molecular arrangement of lipid headgroups and charged polymer segments in layers. A zwitterionic headgroup interacts with two oppositely charged segments, and an ionic headgroup interacts with one charged segment.

trolytes (e.g., negative polyelectrolytes absorbed to a negatively charged outer layer) and thus control the amount adsorbed per layer. The fact that a negatively charged lipid can bind very strongly to a negative surface implies that during deposition the lipid causes severe changes in the polyelectrolyte arrangement. It probably is an essential issue that the use of the LB technique for lipid deposition forces the lipid layer strongly enough to the polyelectrolyte surface to induce appropriate chain rearrangements that enable a net attractive interaction with chains from an internal layer.

Local Interactions. Comparing the PC with the PA headgroup, a lower diffusion coefficient and a higher activation energy is found for the zwitterionic PC group. As discussed above, a lipid charge can bind to segments from either the outer or the second outermost polyelectrolyte layer. Therefore, any lipid charge, whether positive or negative, can lead to an attractive interaction. The difference between the zwitterionic and the ionic lipid diffusion can thus be explained by a different number of binding charges, as shown in Figure 10, where the PC group can interact with two different, oppositely charged polyelectrolyte segments.

The activation energies of the zwitterionic headgroup of the PC are larger than ΔE of the PA group by a factor of about 1.3−1.8. By interpreting the activation energy of the PA headgroup in a molecular picture as the energy required for the release of a charge from an oppositely charged PE monomer, this factor would imply an effective number of 1.3−1.8 charges, which can bind in the case of the PC headgroup. This is somewhat less than a factor of 2 times ΔE(DOPA). One reason for a reduced interaction compared to two independent charges is given by the conformational position of the charges in the PC group. As can be seen from Figure 1, both the negative and the positive charge are sterically less accessible than the PA charge. This will lead to a larger distance between the PC charges and the respective polymer charges and thus cause a reduced interaction per charge. Additionally, the binding energy of each single charge of the PC headgroup can be lowered because of the spatial proximity of both charges such that the interaction of the PC headgroup with the polymer cushion can be described rather by a dipole−dipole interaction, whereas for the single-charged PA group, Coulomb interaction applies. The influence of this latter effect is, however, difficult to estimate because the absolute distances of the charges are not known and a calculation would require estimates of a dielectric constant on a molecular scale.

Conclusions

The electrostatic interactions and their implications for lipid dynamics are investigated in a lipid layer coupled to polyelectrolyte multilayers. By TIR−FRAP pattern bleaching, ultraslow diffusion coefficients on the order of 10^{-12} cm^2/s could be determined not only by order of magnitude but also with a precision of 10%. This enabled the comparison of different systems of varying lipid headgroup charge, lipid chain structure, and last polyelectrolyte layer charge. In the coupled systems studied here, the dynamics of the lipid layer are completely dominated by the electrostatic interaction with the polymer cushion and by the number of lipid charges available for electrostatic interaction. This is suggested by diffusion coefficients and confirmed by the absence of phase transitions and by the corresponding activation energies for diffusion. In this regime of very strong interlayer interactions, the activation energies are interpreted in terms of binding energies of single lipid molecules to polymer segments, which have to be overcome to cause diffusion to other binding sites.

The polyelectrolyte layers can flexibly rearrange when brought into contact with a charged or dipolar lipid layer. Multilayers thus form a type of polymer cushion that optimizes the interaction with the lipids.

Acknowledgment. This work was funded within the Deutsche Forschungsgemeinschaft, Schwerpunkt "Polyelektrolyte mit definierter Molekülarchitektur".

References and Notes

(1) Sackmann, E. *Science (Washington, D.C.)* **1996**, *271*, 43.
(2) Majewski, J.; Wong, J. Y.; Park, C. K.; Seitz, M.; Israelachvili, J. N.; Smith, G. S. *Biophys. J.* **1998**, *75*, 2363.
(3) Sackmann, E.; Tanaka, M. *Trends Biotechnol.* **2000**, *18*, 58.
(4) Wagner, M. L.; Tamm, L. K. *Biophys J.* **2000**, *79*, 1400.
(5) Shen, W. W.; Boxer, S. G.; Knoll, W.; Frank, C. W. *Biomacromolecules* **2001**, *2*, 70.
(6) Yang, Z.; Yu, H. *Langmuir* **1999**, *15*, 1731.
(7) Starr, T. E.; Thompson, N. L. *Langmuir* **2000**, *16*, 10301.
(8) Auch, M.; Fischer, B.; Möhwald, H. *Colloids Surf., A* **2000**, *164*, 39.
(9) Cassier, T.; Sinner, A.; Offenhäuser, A.; Möhwald, H. *Colloids Surf., B* **1999**, *15*, 215.
(10) Decher, G.; Hong, J. D.; Schmitt, J. *Thin Solid Films* **1992**, *210−211*, 831.
(11) Axelrod, D.; Koppel, D. E.; Schlessinger, J.; Elson, E.; Webb, W. W. *Biophys. J.* **1976**, *16*, 1055.
(12) Smith, B. A.; McConnell, H. M. *Proc. Natl. Acad. Sci. U.S.A.* **1978**, *75*, 2759.
(13) Davoust, J.; Devaux, P. F.; Leger, L. *EMBO J.* **1982**, *1*, 1233.
(14) Wright, L. L.; Palmer, A. G., III; Thompson, N. L. *Biophys. J.* **1988**, *54*, 463.
(15) Thompson, N. L.; Pearce, K. H.; Hsieh, H. V. *Eur. Biophys. J.* **1993**, *22*, 367.
(16) Vaz, W. L. C. *Biophys. Chem.* **1994**, *50*, 139.
(17) Miehlich, R.; Gaub, H. E. *Rev. Sci. Instrum.* **1993**, *64*, 2632.
(18) Decher, G.; Lvov, Y.; Schmitt, J. *Thin Solid Films* **1994**, *244*, 772.
(19) Decher, G. *Science (Washington, D.C.)* **1997**, *277*, 1232.
(20) Farhat, T.; Yassin, G.; Dubas, S. T.; Schlenoff, J. B. *Langmuir* **1999**, *15*, 6621.
(21) Jacobson, K. *Cell Motil.* **1983**, *3*, 367.
(22) Adalsteinsson T.; Yu, H. *Langmuir* **2000**, *16*, 9410.
(23) Wang, L.; Schönhoff, M. Unpublished results.
(24) Evans, E.; Sackmann, E. *J. Fluid Mech.* **1988**, *194*, 553.
(25) Lösche, M.; Schmitt, J.; Decher, G.; Bouwman, W. G.; Kjaer, K. *Macromolecules* **1998**, *31*, 8893.
(26) Klitzing, R. v.; Möhwald, H. *Thin Solid Films* **1996**, *284−285*, 352.
(27) Decher, G.; Schmitt, J. *Prog. Colloid Polym. Sci.* **1992**, *89*, 160.
(28) Wang, L.; Schönhoff, M. To be submitted for publication.
(29) Leporatti, S.; Gao, C.; Voigt, A.; Donath, E.; Möhwald, H. *Eur. Phys. J. A* **2001**, *5*, 13.
(30) Merkel, R.; Sackmann, E.; Evans, E. *J. Phys. (Orsay, Fr)* **1989**, *50*, 1535.
(31) Lalchev, Z. I.; Wilde, P. J.; Clark, D. C. *Colloids Surf.* **1994**, *167*, 80.
(32) Galla, H. J.; Hartmann, W.; Theilen, U.; Sackmann, E. *J. Membr. Biol.* **1979**, *48*, 215.
(33) Graf, K.; Riegler, H. *Colloids Surf., A* **1998**, *131*, 215.
(34) Sukhorukov, G. B.; Donath, E.; Lichtenfeld, H.; Knippel, E.; Knippel, M.; Budde, A.; Möhwald, H. *Colloids Surf., A* **1998**, *137*, 253.